IJE TRANSACTIONS C: Aspects Vol. 26, No. 12, (December 2013) 1495-1504

International Journal of Engineering

Journal Homepage: www.ije.ir

Stress Patterns in Single Deck Floating Roofs Subjected to Ground Motion Accelerations

R. Shabani*

Department of Mechanical engineering, Islamic Azad University Shabestar Branch, Shabestar, Iran

PAPER INFO

Paper history:
Received 26 February 2013
Received in revised form 28 April 2013
Accepted 20 June 2013

Keywords:
Cylindrical Tank
Stress Pattern
Earthquake
Floating Roof

ABSTRACT

This paper investigates the induced stresses in circular single deck roofs floating on seismically excited storage tanks. Equations of motion are derived using variational principle. Response of deck floating roofs is evaluated for two different classes of ground motions; near-source and long-period far-field records. Besides time histories and frequency contents for a specific tank, peak value diagrams of stress for tanks with different radii are illustrated. Results indicate two critical locations in the deck roofs: one near the center of the roof and the other along the deck-pontoon interface. It is shown that near-source ground motions produce larger stresses at the inner critical radius of the deck but far-field ground motions lead to larger stresses in deck-pontoon interface. These critical locations and their stress dependencies have not been reported in previous works. The results could have practical implications in the design process of floating roofed cylindrical tanks.

doi: *10.5829/idosi.ije.2013.26.12c.10*

1. INTRODUCTION

Floating roofed storage tanks are inseparable parts of large scale liquid storage facilities such as oil, petroleum and petrochemical industries due to their economic and environmental advantages. Floating roofs eliminate evaporation by covering the exposed liquid surface, thus reducing material loss and air pollution. Moreover, the possibility of fire hazard in highly flammable hydrocarbon vapors due to sources like earthquakes, static electricity, cigarette smoking, etc. is considerably diminished [1].

Liquid sloshing has been observed to be largely responsible for the floating roof damages in the past earthquakes [2]. Thus the inclusion of fluid-structure interaction in design and analysis of floating roofed tanks subjected to ground motions is essential. Sakai and coworkers [3] were one of the first researchers to calculate the natural frequencies floating roofs by introducing variational approach to the problem. Isshiki and Nagata [4] derived the extended Hamiltonian principle for a floating plate by combining Hamilton's principle for plate and Kelvin's principle for water. Amabili and Kwak [5] implemented Hankel transformation in Rayleigh-Ritz method to analyze the free vibration of circular plates with any form of uniform boundary conditions. Matsui employed Fourier-Bessel series to derive the linear equations of motion for a base excited tank with a double deck [6] and single deck [7] floating roof and compared the results with those of unroofed tank. Utilizing a specific seismic input, he demonstrated the effect of different modes on the roof deflection, liquid pressure and bending stresses. Nagaya et al. [8] performed shaking table tests to reveal the vibrational characteristics of roofs and showed the strong dependency of damping ratio on roof type. Epstein [9] analyzed the effect of structural parameters on the stresses in single deck floating roofs using a shooting method. Kwak and Kim [10] used non-dimensionalized added mass factors to investigate the effect of fluid on natural frequencies of axisymmetric circular plates of various boundary conditions, and showed the decreasing fluid effect with respect to mode number. Sun et al. [11] carried out a static finite element stress analysis in a single deck floating roof subjected to water ponding. Using an iterative method, they demonstrated the vulnerability of deck-pontoon interface. Similar conclusions were also drawn by Shabani et al. [12]. They used a variational approach to evaluate the equilibrium conditions between the elastic

*Corresponding Author Email: r.shabani@Urmia.ac.ir (R. Shabani)

and buoyant forces and determined the contribution of membrane and flexural constituents to the overall roof stiffness. It was shown that modeling of the deck plate as a flexural element rather than a membrane, by eliminating the need for nonlinear analysis, gives reasonable results for deflections and stresses in the deck plate. Golzar et al. [13], using extended Hamilton's principle, presented a comprehensive set of results predicting behavior of tanks with double deck roofs when excited by different types of earthquakes. It was concluded that while long-period far-field ground motions control the free board height, near-source records give higher values for lateral forces and overturning moments induced on the tank. Later, Shabani and Golzar [14] derived the nonlinear equation of motion for a uniform plate floating on top of a seismically excited cylindrical tank and showed the suppressing effect of nonlinearities on the sloshing heights for a wide range of tank dimensions. Following on, Shabani et. al [15] have shown that accounting for large deflections could substantially reduce the wave elevation for near resonance harmonic excitations. Evaluating the response of the nonlinear model for increasing amplitudes of harmonic excitations gives rise to the appearance of super harmonics and chaotic vibrations in the response. Response of base isolated cylindrical tanks, with and without roof, to earthquake excitations was the subject of a comprehensive experimental study by De Angelis et al. [16]. They verified the results by simple numerical methods and showed the favorable effects of base isolators and floating roofs on reducing the wall pressures and oscillation amplitudes, respectively.

This study intends to provide a more conclusive and comprehensive result set on the dynamic response of single-deck floating roofs under seismic excitation. Applying the Hamilton's variational principle on the floating roof and contained liquid simultaneously, the response of roofed storage tanks to different earthquakes including near-source and far-field records are investigated. Numerical integration is used to evaluate the stresses of the roof. Stress patterns produced in the deck of the floating roof and in the pontoon deck interface. Moreover, effect of earthquake type is studied for a practical range of tank dimensions. The results may prove useful in design considerations.

2. MATHEMATICAL MODEL

Figure 1 illustrates a cylindrical tank of radius R filled to a height H with an incompressible liquid of density ρ and equipped with an elastic floating roof. The conventional floating roofs can be categorized into two types: single deck and double deck where the single deck type is investigated in this paper. Single deck roofs

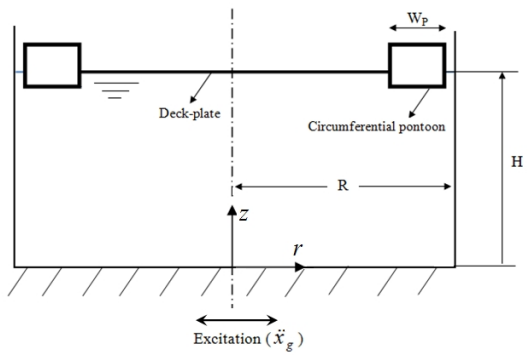

Figure 1. Cylindrical liquid storage tank with a single deck floating roof

are composed of a circumferential buoyant ring (pontoon) with relatively large stiffness surrounding an inner circular plate (deck) with small thickness and stiffness. Tank wall and bottom are assumed rigidly excited by the unidirectional ground excitation, $\ddot{X}_g$.

Laplace equation together with the impermeability and kinematic boundary conditions may be used to fully define the movement of the liquid inside the enclosed tank volume.

$$\nabla^2 \Phi = 0 \qquad 0 \le r \le R,\ 0 \le \theta \le 2\pi \tag{1}$$

$$\frac{\partial \Phi}{\partial z} = 0 \qquad z = 0 \tag{2}$$

$$\frac{\partial \Phi}{\partial r} = \dot{x}_g \qquad r = R \tag{3}$$

where Φ is the velocity potential function and *(r, θ, z)* denotes the cylindrical coordinates. Imposing these conditions, the velocity potential is obtained in the following form [15]:

$$\Phi(r, z, \theta) = r\dot{x}_g \cos\theta + \Phi_0$$

$$\Phi_0 = \sum_{k=1}^{\infty} A_k \frac{J_1\left(\frac{\varepsilon_k r}{R}\right)\cosh\left(\frac{\varepsilon_k z}{R}\right)}{J_1(\varepsilon_k)\cosh\left(\frac{\varepsilon_k H}{R}\right)}\cos\theta \tag{4}$$

where A_ks are the unknown time dependent shape factors, J_1 denotes the Bessel function of the first kind of order one and eigenvalues of the velocity potential, ε_ks are the roots of equation $J_1(\varepsilon_k)=0$. Lateral vibration of the floating roof can be considered as a weighted summation of free vibration mode shapes of a free-edge circular plate:

$$\eta(r, \theta, t) = \sum_{i=1}^{\infty} B_i(t) X_i(r) \cos\theta \tag{5}$$

where B_i denote the generalized coordinates and X_i the radial mode shapes consisting of rigid and elastic modes [17]:

$$X_1(r)=\frac{r}{R}$$
$$X_i(r)=\left[\alpha_i J_1\left(k_i\frac{r}{R}\right)+\beta_i I_1\left(k_i\frac{r}{R}\right)\right] \quad (6)$$

K_i represent the radial eigenvalues of the free-edge circular plate and I_1 denotes the modified Bessel function of the first kind of order one. Bearing in mind that the roof and liquid stay in complete contact, the assembled Lagrangian of the coupled system, accounting for the kinetic and potential energies, is written in form of the sum of roof Lagrangian L_R and liquid Lagrangian L_l [18]:

$$\begin{aligned}L&=L_R+L_l\\&=\int_{r=0}^{R}\int_{\theta=0}^{2\pi}\left\{\frac{1}{2}M_R\dot{\eta}^2-\frac{1}{2}D_R\left[\begin{array}{l}\left(\frac{\partial^2\eta}{\partial r^2}\right)^2+\left(\frac{1}{r}\frac{\partial\eta}{\partial r}+\frac{1}{r^2}\frac{\partial^2\eta}{\partial\theta^2}\right)^2\\+2\nu\left(\frac{\partial^2\eta}{\partial r^2}\right)\left(\frac{1}{r}\frac{\partial\eta}{\partial r}+\frac{1}{r^2}\frac{\partial^2\eta}{\partial\theta^2}\right)\\+2(\upsilon-1)(\frac{1}{r}\frac{\partial^2\eta}{\partial r\partial\theta}-\frac{1}{r^2}\frac{\partial\eta}{\partial\theta})\end{array}\right]\right\}rdrd\theta\\&+\int_{r=0}^{R}\int_{\theta=0}^{2\pi}\rho_L\left[-\frac{1}{2}\left(\frac{\partial\Phi_0}{\partial z}\right)\Phi_0+\frac{\partial\eta}{\partial t}\Phi-\frac{1}{2}g\eta^2\right]rdrd\theta\end{aligned} \quad (7)$$

where M_R and D_R denote the mass and rigidity of the roof. Making use of the Hamiltonian principle, the equation of motion of roof is obtained in the following matrix form:

$$M_R[P]\{\ddot{B}\}+(D_R[Q]+\rho_L g[U])\{B\}+\rho_L[T]\{\dot{A}\}+\rho_L\ddot{X}_g\{F\}=0 \quad (8)$$

$$[T^t]\{\dot{B}\}-[S]\{A\}=0 \quad (9)$$

Elements of matrices P, Q, U, F, S and T are specified as follows:

$$\begin{aligned}P_{ij}&=\int_0^R X_iX_j rdr\\Q_{ij}&=\int_0^R X_i'X_j''rdr+\int_0^R\left(\frac{1}{r}X_i'-\frac{1}{r^2}X_i\right)\left(\frac{1}{r}X_j'-\frac{1}{r^2}X_j\right)(3-2\upsilon)rdr\\&+\int_0^R X_i''\left(\frac{1}{r}X_j'-\frac{1}{r^2}X_j\right)+X_j'\left(\frac{1}{r}X_i'-\frac{1}{r^2}X_i\right)\upsilon rdr\\U_{ij}&=\int_0^R X_iX_j rdr\\T_{ij}&=\int_0^R X_i\frac{J_1(\varepsilon_j r/R)}{J_1(\varepsilon_j)}rdr\\F_i&=\int_0^R rX_i rdr\\S_{ij}&=\frac{R}{2}\varepsilon_j\tanh\left(\varepsilon_j\frac{H}{R}\right)\left(1-\frac{1}{\varepsilon_j^2}\right)\end{aligned} \quad (10)$$

Unifying Equations (8) and (9) rolls out the shape factor A:

$$\begin{aligned}&\left(M_R[P]+\rho_L[T][S^{-1}][T^t]\right)\{\ddot{B}\}+\\&\quad(D_R[Q]+\rho_L g[U])\{B\}+\rho_L\ddot{X}_g\{F\}=0\end{aligned} \quad (11)$$

The equation suggests that both dynamic and static couplings exist between the roof and oscillating fluid, resulting in a coupled set of equations. The mass matrix in Equation (11) is composed of two parts: $M_R[P]$ accounting for the presence of floating plate and $\rho_L[T][S^{-1}][T^t]$, representing the added inertial effect of the liquid. Likewise, stiffness matrix is composed of $D_R[Q]$ accounting for the plate stiffness and $\rho_L g[U]$ representing the added stiffness due to fluid co-vibration.

By truncating Equations (4) and (5) to limited numbers n and m respectively, the obtained set of equations may be solved to yield the generalized coordinates and consequently plate deflection and liquid velocity potential. Moreover, radial and circumferential bending moments resulting in the bending stresses in roof cross-section are calculated by the following formulae:

$$M_r=-D_R\left(\frac{\partial^2\eta}{\partial r^2}+\upsilon\left[\frac{1}{r}\frac{\partial\eta}{\partial r}+\frac{1}{r^2}\frac{\partial^2\eta}{\partial\theta^2}\right]\right) \quad (12)$$

$$M_\theta=-D_R\left(\left[\frac{1}{r}\frac{\partial\eta}{\partial r}+\frac{1}{r^2}\frac{\partial^2\eta}{\partial\theta^2}\right]+\upsilon\frac{\partial^2\eta}{\partial r^2}\right) \quad (13)$$

3. EXCITATION CHARACTERISTICS

In order to evaluate the dynamic behavior of seismically excited roofed tank, following ground motion data were utilized as base excitations: 90 component of 1995 Kobe earthquake at Japan recorded at Nishi-Akashi station (KOBE/NIS000),180 component of 1940 Imperial Valley earthquake recorded at El Centro station (IMPVALL/I-ELC180), EW component of 2003 Tokachi-oki earthquake recorded at Tomakomai station (HKD1290309260450EW), and EW component of 2011 Tohoku earthquake (Eastern Japan earthquake) recorded at Chiba station (CHB0091103111446). Table 1 shows the duration, peak ground acceleration and epicentral distance of earthquake records. Time histories and Fourier decomposition of the records are shown in Figures 2 and 3.

TABLE 1. Seismic data used in this study

Input ground motion	Duration (s)	PGA (g)	Epicentral Distance (km)
Kobe (1995)	40	0.4862	8.7
Imperial Valley (1940)	40	0.3130	13
Tokachi-oki (2003)	290	0.0800	227
Tohoku (2011)	300	0.1397	364

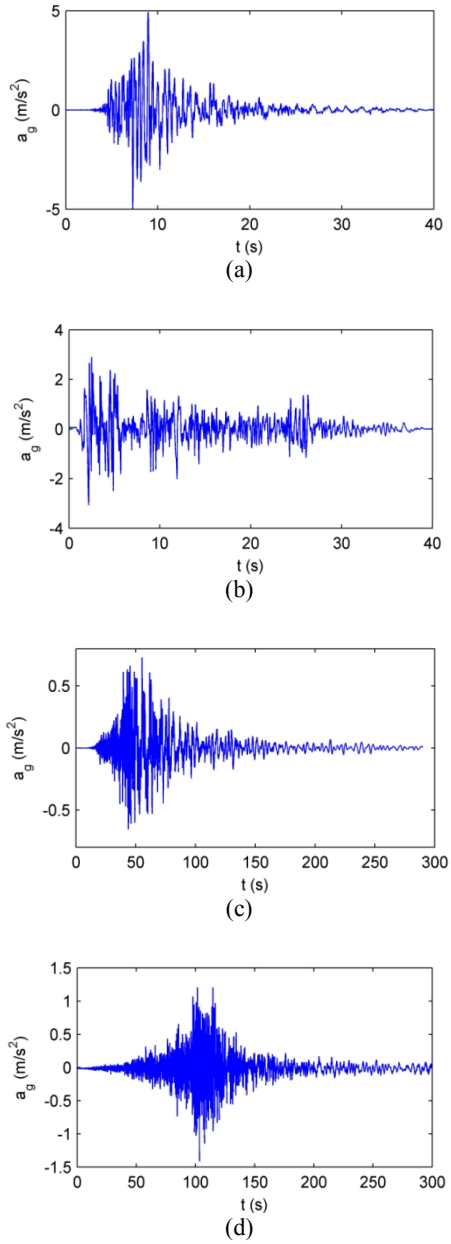

Figure 2. Time histories of ground motions, (a) Kobe, (b) Imperial Valley, (c) Tokachi-oki, (d) Tohoku

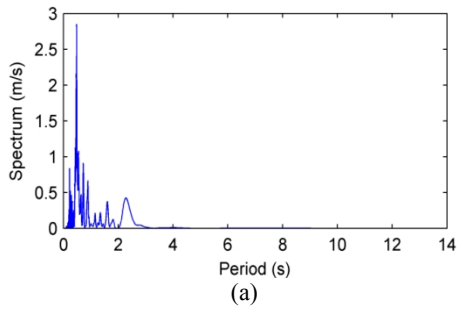

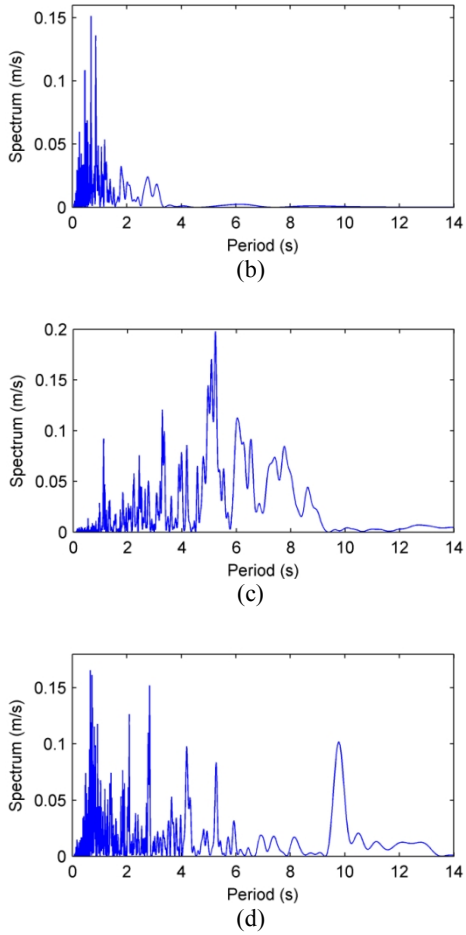

Figure 3. Fast Fourier Transform (FFT) of ground motions (a) Kobe, (b) Imperial Valley, (c) Tokachi-oki, (d) Tohoku

Kobe and Imperial Valley ground motions possessing rather similar frequency content (containing spectral peaks at low periods) are classified as near-source earthquakes. On the other hand, Tokachi-oki and Tohoku with broad band frequency content are classified as long period, far-field records. Near-source earthquakes act in a shorter time interval but impose larger accelerations to the structures compared to long period, far-field earthquakes.

4. SIMULATION RESULTS

In this study, recordings of the aforementioned earthquakes are used as base excitation for a wide range of tank dimensions with the geometrical and material properties shown in Table 2.

Natural periods of the coupled system, obtained from the free vibration analysis of the system are shown in Figure 4.

TABLE 2. Geometrical and material properties of tank with a single-deck floating roof

Tank height (H)	15 m
Tank Radius (R)	25 m
Pontoon width (W_P)	3 m
Deck areal mass density (M_d)	58 kg/m^2
Pontoon areal mass density (M_P)	173 kg/m^2
Pontoon bending rigidity (D_P)	2.70×10^5 kN.m
Deck plate thickness (h_D)	4.5 mm
Liquid density (ρ)	800 kg/m^3
Damping ratio (ζ)	0.005
Poisson's ratio (v)	0.3
Adopted modes for roof vibration (n)	29
Adopted modes for liquid sloshing (m)	33

Even though the equations were derived for an ideally undamped system, the actual structures show a rate of energy dissipation which may be attributed to various sources like viscous liquid-wall interaction or/and friction between roof and wall. In order to account for these terms, damping matrix C is added to Equation (11) to yield the following more practical equation:

$$\left(M_R[P]+\rho_L[T][S^{-1}][T^t]\right)\{\ddot{B}\}+[C]\{\dot{B}\} \\ \left(D_R[Q]+\rho_L g[U]\right)\{B\}+\rho_L \ddot{X}_g\{F\}=0 \quad (14)$$

The stiffness proportional damping is adopted with the modal damping ratio shown in Table 2. Selected value (0.01) is in accordance with the experimental findings of Nagaya et al. [8] where it was stated that the Rayleigh damping was appropriate for single deck roofs. In numerical simulations, Newmark's average acceleration method [19] is employed to solve Equation (14).

4. 1. Effect of Near-Source Excitations Kobe and Imperial Valley Response of the storage tank to Near-Source excitations Kobe and Imperial Valley is depicted in the following figures. Figures 5b and 6b show the multiple local peaks in the stress diagrams among which the near center peak is the most vulnerable one (central critical radius). Fourier decomposition of critical radial stress reveals that the oscillation of critical stress is substantially affected by the activation of higher modes (Figures 5c and 6c).

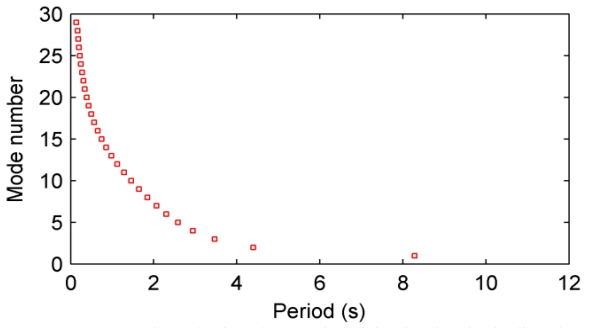

Figure 4. Natural periods of a tank with single deck floating roof

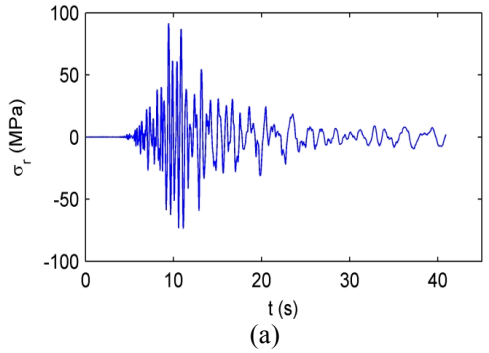

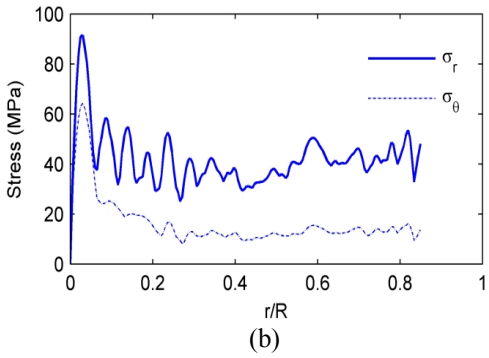

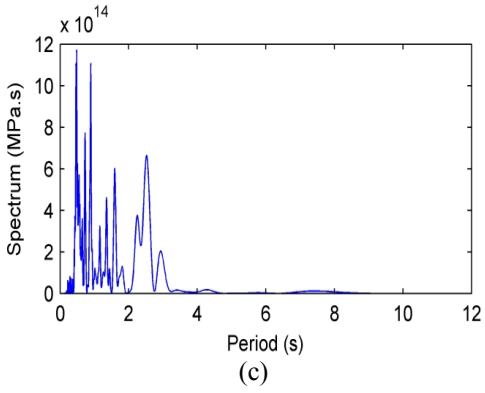

Figure 5. Response to Kobe excitation, (a) Time history of radial stress, (b) Maximum bending stresses, (c) Frequency content of radial stress

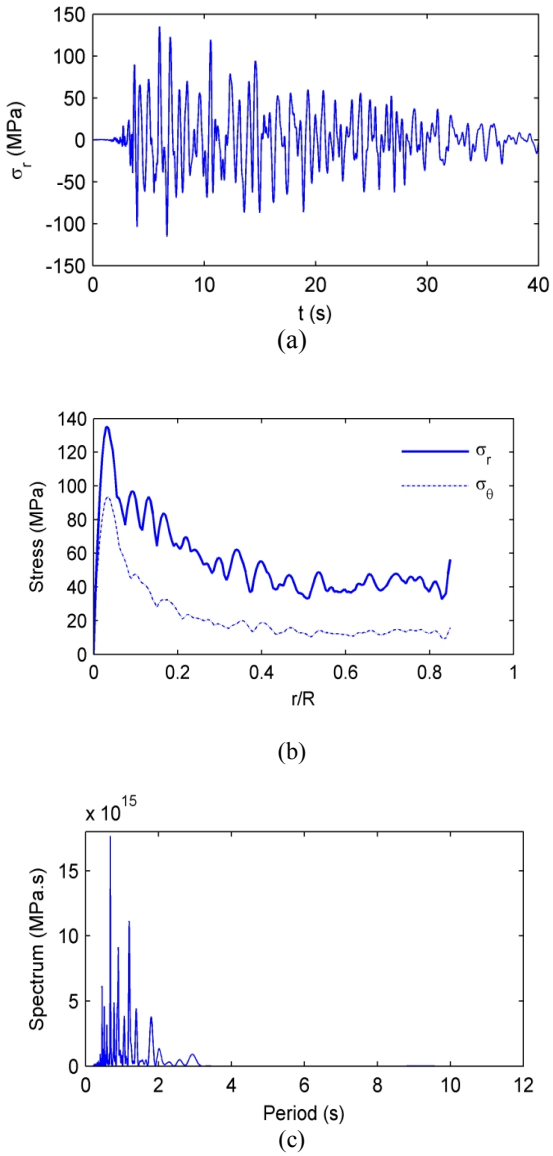

Figure 6. Response to Imperial Valley excitation, (a) Time history of radial stress, (b) Maximum bending stresses, (c) Frequency content of radial stress

4. 2. Effect of Far-Field Excitations Tokachi-oki and Tohoku Dynamic behavior of deck roof subjected to Tokachi-oki earthquake is shown in Figure 7. Despite the near-source excitations, here the amplitude of bending stress shows a low rate of dissipation (Figure 7a). Maximum value of bending stress occurs along the deck-pontoon interface while the value of stress at other radii is considerably lower (Figure 7b). Fourier decomposition of radial stress are dominated by the first mode with a little contribution of second mode (Figure 7c) which is due to the rich content of earthquake at higher periods and its low content near the lower periods.

Response of the deck floating roof to Tohoku earthquake is depicted in Figure 8. Roof shows an oscillatory motion till the end of the earthquake producing considerable bending stresses in the roof cross section (Figure 8a). Stresses induced within the roof share characteristics of both near-source excitations Kobe and Imperial Valley and Far-field Tokachi-oki as the Tohoku earthquake possesses rich frequency content at both high and low periods. As a result, two critical radii are present in the graphs; central critical radius and deck-pontoon interface (Figure 8b). Bending stress oscillates mainly in the first mode but effect of second mode is also apparent in the stress (Figure 8c).

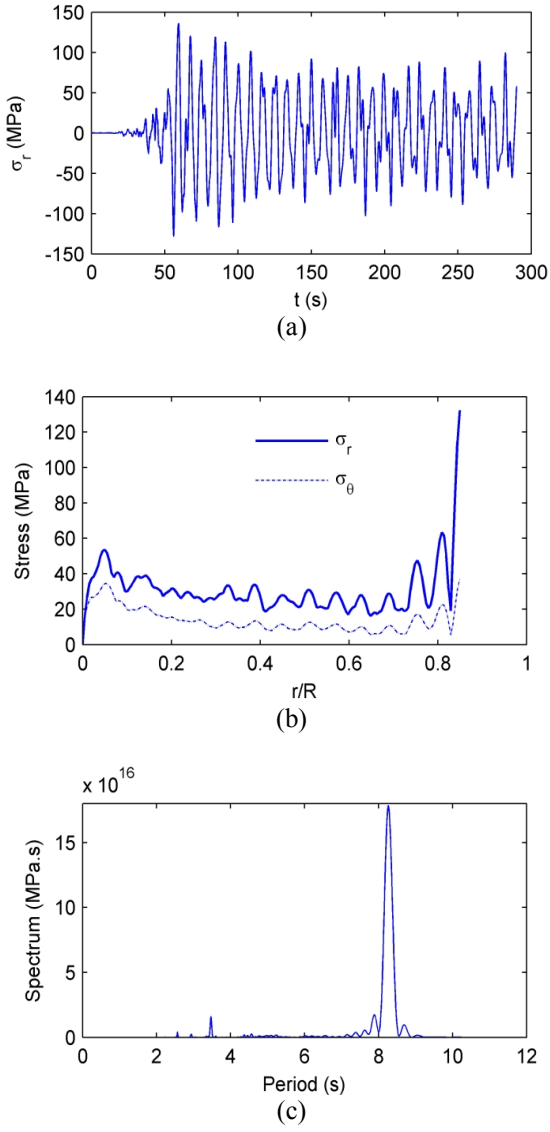

Figure 7. Response to Tokachi-oki excitation, (a) Time history of radial stress, (b) Maximum bending stresses, (c) Frequency content of radial stress

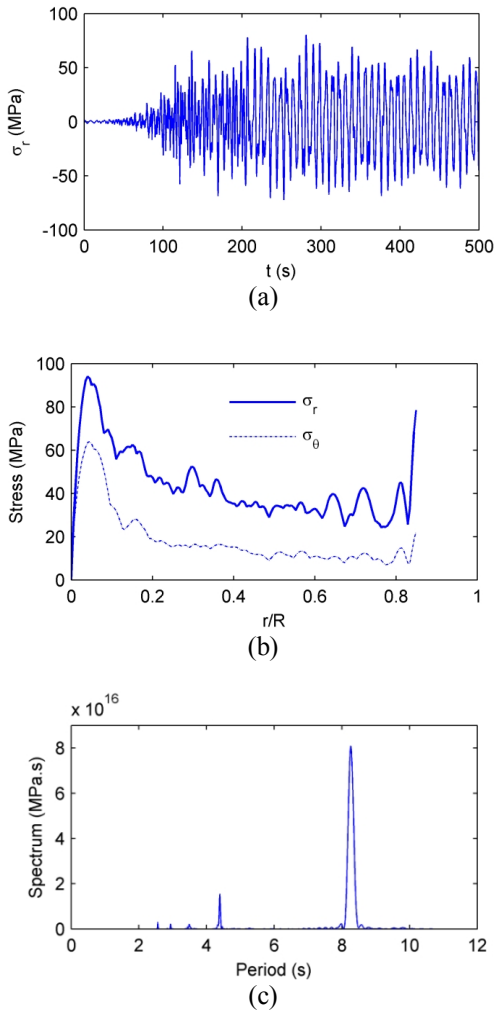

Figure 8. Response to Tohoku excitation, (a) Time history of radial stress, (b), Maximum bending stresses, (c) Frequency content of radial stress

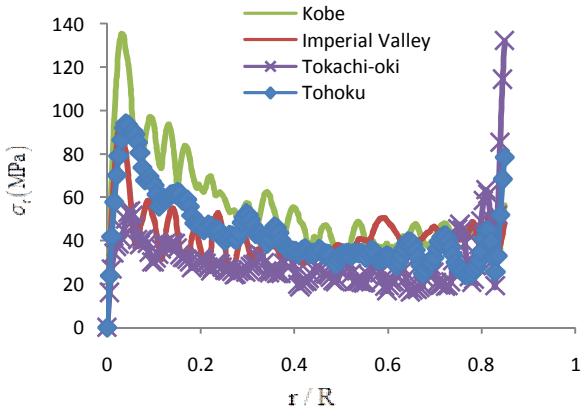

Figure 9. Radial bending stress in single deck roof for different earthquakes

4. 3. Relative Effect of Earthquakes on the Response of the Deck Roofs For the sake of comparison, radial stresses in the deck plate, caused by the four mentioned ground motions are plotted altogether in Figure 9. Stresses in the pontoon were assumed zero, and thus are not plotted here. It is seen that near-source ground motions Kobe and Imperial Valley produce large stresses in the central critical radius while far-field, long period earthquake Tokahci-oki and Tohoku result in large stresses along the deck-pontoon interface. Moreover, Tohoku earthquake imposes considerably large stresses at the central critical radius as its frequency content is rich at low periods as well as high periods activating higher modes of vertical deflection of the deck plate. As observed in the previous figures, circumferential stresses have the same pattern as the radial stresses but have smaller value.

Effect of tank radius on the bending stresses produced within the deck floating roof is illustrated in Figure 10. The radius of the roof and tank is swept from 20 to 40 meters to include the typical range of tanks used in the petroleum industries. Note that other properties of the coupled system are kept intact. Radial and circumferential stresses at the two most vulnerable radii are plotted with respect to the radius of the tank. Strong material of the near-source earthquakes Kobe and Imperial Valley resulted in high modes of the coupled system being activated. Thus, the stresses at the central critical radius are significantly influenced by the higher modes, which taken larger values compared to the case of far-field excitations. In contrary, for the stresses occurred along the deck-pontoon interface is valid. The oscillation of these stresses is mainly controlled by the fundamental period of the system so far-field earthquakes which possess strong content at high periods render greater values at this radius. The stresses along the deck-pontoon interface show an overall descending trend with respect to radius. Consequently, for sufficiently wide tanks, deck-pontoon interface is no longer a high-risk critical point compared to the central critical radius. In conclusion, the design criteria for the strength of the deck plate may be divided into two parts; strength at the central radii which should be determined by the characteristics of near-source ground motions, and bending strength along its connection with annular pontoon which should be predicted by the probable hazards of far-field quakes.

5. CONCLUSION

Stress analysis of single deck floating roofs with circumferential pontoon in seismically excited storage tank was derived using Hamiltonian variational principle. Two classes of earthquakes, near-source and long-period far-field were utilized in the simulations. Evaluation of response revealed the presence of higher

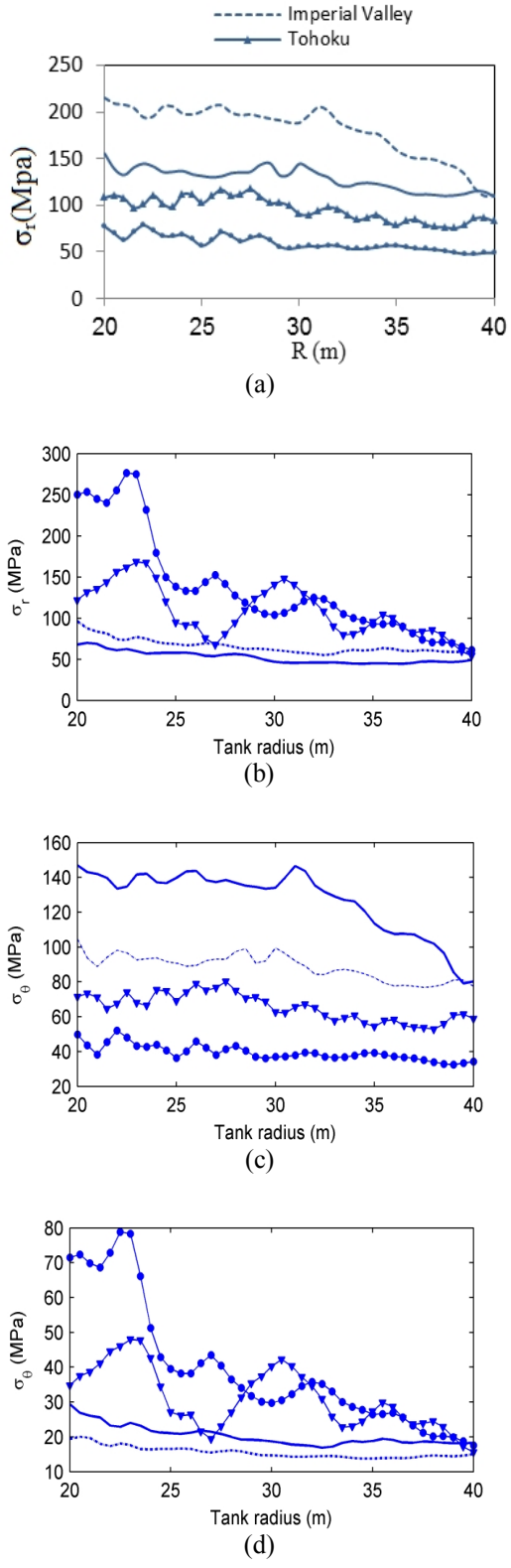

Figure 10. Effect of earthquakes on tanks with different dimensions, (a) radial stress at central critical radius, (b) Radial stress at deck-pontoon interface, (c) Circumferential stressat central critical radius, (d) Circumferential stress at deck-pontoon interface

modes was considerable in the stresses especially at central parts of the roof. Single deck roofs were prone to failure when excited by far-field ground motion as well as near-source ones. Two critical locations were witnessed in the deck roofs: one near the center of the roof (more susceptible to near source earthquakes) and the other along the deck-pontoon interface (more susceptible to far-field earthquakes). Results suggest that near-source ground motions produce larger stresses at the inner critical radius of the deck, but far-field ground motions lead to larger stresses in deck-pontoon interface. It is concluded that bending stress evaluation requires consideration of both near-source and far-field hazards.

7. REFERENCES

1. Chang, J. I. and Lin, C.-C., "A study of storage tank accidents", ***Journal of Loss Prevention in the Process Industries***, Vol. 19, No. 1, (2006), 51-59.
2. Hatakeyama, K., Zama, S., Nishi, H., Yamada, M., Hirokawa, Y., and Inoue, R., "Long-period strong ground motion and damage to oil storage tanks due to the 2003 tokachi-oki earthquake", ***Journal of the Seismological Society of Japan. Second Series***, Vol. 57, No. 2, (2004), 83-103.
3. Sakai, F., Nishimura, M. and Ogawa, H., "Sloshing behavior of floating-roof oil storage tanks", ***Computers & Structures***, Vol. 19, No. 1, (1984), 183-192.
4. Isshiki, H. and Nagata, S., "Variational principles related to motions of an elastic plate floating on a water surface", ***Journal-Kansai Society of Naval Architects Japan***, (2000), 79-86.
5. Amabili, M. and Kwak, M., "Free vibrations of circular plates coupled with liquids: Revising the lamb problem", ***Journal of Fluids and Structures***, Vol. 10, No. 7, (1996), 743-761.
6. Matsui, T., "Sloshing in a cylindrical liquid storage tank with a floating roof under seismic excitation", ***Journal of Pressure Vessel Technology***, Vol. 129, No. 4, (2007), 557-566.
7. Matsui, T., "Sloshing in a cylindrical liquid storage tank with a single-deck type floating roof under seismic excitation", ***Journal of Pressure Vessel Technology***, Vol. 131, No. 2, (2009).
8. Nagaya, T., Matsui, T. and Wakasa, T., "Model tests on sloshing of a floating roof in a cylindrical liquid storage tank under seismic excitation", ASME. (2008).
9. Epstein, H. I., "Stresses and displacements for floating pan roofs", ***Computers & structures***, Vol. 15, No. 4, (1982), 433-438.
10. Kwak, M. and Kim, K., "Axisymmetric vibration of circular plates in contact with fluid", ***Journal of Sound and Vibration***, Vol. 146, No. 3, (1991), 381-389.
11. Sun, X., Liu, Y., Wang, J. and Cen, Z., "Stress and deflection analyses of floating roofs based on a load-modifying method", ***International Journal of Pressure Vessels and Piping***, Vol. 85, No. 10, (2008), 728-738.
12. Shabani, R., Tariverdilo, S., Salarieh, H. and Rezazadeh, G., "Importance of the flexural and membrane stiffnesses in large deflection analysis of floating roofs", ***Applied Mathematical Modelling***, Vol. 34, No. 9, (2010), 2426-2436.
13. Golzar, F., Shabani, R., Tariverdilo, S. and Rezazadeh, G., "Sloshing response of floating roofed liquid storage tanks subjected to earthquakes of different types", ***Journal of Pressure Vessel Technology***, Vol. 134, No., (2012), 051801.

14. Shabani, R. and Golzar, F., "Large deflection analysis of floating roofs subjected to earthquake ground motions", ***Nonlinear Analysis: Real World Applications***, Vol. 13, No. 5, (2012), 2034-2048.

15. Shabani, R., Tariverdilo, S. and Salarieh, H., "Nonlinear vibrations and chaos in floating roofs", ***Journal of Computational and Nonlinear Dynamics***, Vol. 7, No. 2, (2012).

16. De Angelis, M., Giannini, R. and Paolacci, F., "Experimental investigation on the seismic response of a steel liquid storage tank equipped with floating roof by shaking table tests", ***Earthquake Engineering & Structural Dynamics***, Vol. 39, No. 4, (2010), 377-396.

17. William, T. T. and Marie, D. D., "Theory of vibration with applications", ***New Jersey***, (1998).

18. Meirovitch, L., "Principles and techniques of vibrations", Prentice Hall New Jersey, (1997).

19. Chopra, A. K., "Dynamics of structures: Theory and applications to earthquake engineering", Prentice Hall Saddle River, (2001).

Stress Patterns in Single Deck Floating Roofs Subjected to Ground Motion Accelerations

R. Shabani

Department of Mechanical engineering, Islamic Azad University Shabestar Branch, Shabestar, Iran

P A P E R I N F O

Paper history:
Received 26 February 2013
Received in revised form 28 April 2013
Accepted 20 June 2013

Keywords:
Cylindrical Tank
Stress Pattern
Earthquake
Floating Roof

چکیده

در این مقاله آنالیز تنش سقف‌های شناور مخازن استوانه‌ای نگه‌داری مایعات تحت تحریک زلزله مورد بررسی قرار گرفته است. معادلات دینامیکی سیستم با استفاده از اصل حساب تغییرات استخراج شده و سپس پاسخ سقف مخزن به ازاء دونوع زلزله نزدیک میدان و پریود باند دور میدان مورد بررسی قرار گرفته است. در نتایج ارائه شده علاوه بر پاسخ زمانی و محتوای فرکانسی پاسخ مقادیر تنش بیشینه برای مخازن با اندازه‌های مختلف نیز ارائه گردیده است. نتایج ارائه شده نشان دهنده‌ی وجود دو نقطه‌ی بحرانی در ورق سقف بوده که یکی در نزدیکی مرکز و دیگری مربوط به محل تماسی ورق سقف به رینگ کناری می‌باشد. نتایج نشان می‌دهند که زلزله‌های نزدیک میدان باعث بروز تنش‌های بحرانی در نزدیکی مرکز ورق و زلزله‌های دور میدان پریود بالا باعث ایجاد تنش‌های بحرانی در محل تماس ورق به رینگ کناری می‌گردند. نواحی بحرانی فوق و وابستگی تنش‌های گزارش شده در آنها در دیگر مقالات گزارش نشده و لذا نتایج به دست آمده می توانند در مراحل طراحی مخازن استوانه در مناطق زلزله‌خیز مورد استفاده قرار گیرند.

doi: *10.5829/idosi.ije.2013.26.12c.10*